J. Fluid Mech. (1965), *vol.* 22, *part* 2, *pp.* 371–383
Printed in Great Britain

Vortex formation in a free boundary layer according to stability theory

By A. MICHALKE

Deutsche Versuchsanstalt für Luft- und Raumfahrt,
Institut für Turbulenzforschung, Berlin

(Received 10 October 1964)

An attempt is made to explain the formation of vortices in free boundary layers by means of stability theory using a hyperbolic-tangent velocity profile. The vorticity distribution of the disturbed flow, as obtained by the inviscid linearized stability theory, is discussed. The path lines of particles which are initially placed along straight lines parallel to the x-axis are calculated. Lines connecting the positions of these particles give an impression of the instant shape of the disturbed flow. With increasing time the boundary layer becomes thinner in certain regions and thicker in others. A special line—originally positioned at the critical layer—shows in the thicker region a tendency to roll up. Also extrema of the vorticity are located there. Finally, these results are compared with those which can be expected from the non-linear Helmholtz equation. Disagreement is found in the neighbourhood of the critical layer. Using the non-linear stability theory of Stuart up to the third-order terms, the vorticity distribution shows the tendency expected from the non-linear equation.

1. Introduction

The boundary layers of jets and wakes are not bounded by walls and are therefore called free boundary layers. Considering the laminar-turbulent transition, it is known from smoke experiments (see, for instance, Wille 1963) that the free laminar boundary layer can roll up into vortices and turbulence starts where the vortices decay. These vortices, however, are certainly not of the well-known potential type, but as real vortices they may be defined by the existence of a local concentration of vorticity as, for instance, is found in a Hamel–Oseen vortex. For large Reynolds numbers the flow in a free boundary layer is approximately parallel. Therefore results obtained for parallel flows may then be applicable for free boundary layers.

The problem of vortex formation was first considered by Helmholtz (1868). He came to the conclusion that a disturbed free boundary layer would roll up. Later on, Lord Rayleigh (1880) was able to show that a velocity profile with an inflexion point is unstable to certain small wavy disturbances, if the viscosity is neglected. Lin (1955) gave physical explanations for this behaviour: a disturbance of the vorticity which corresponds to a velocity profile with an inflexion point can grow in time as a consequence of the mutual induction of all vortex elements. This is an inviscid effect, and the presence of viscosity will only be of damping influence.

Now, free boundary layer profiles have always one or more inflexion points. Thus, for large Reynolds numbers, amplified disturbances can always exist, and, if they exist, we can suppose after Helmholtz that the free boundary layer should roll up. Furthermore, if vortices of the kind described above are formed during the rolling-up process, we have to expect concentrations of vorticity there.

To prove this hypothesis about the formation of vortices in free boundary layers, some steps have already been taken. First, theoretical and experimental investigations by Lessen (1950), by Esch (1957), Tatsumi & Kakutani (1958), as well as by Sato (1960), by Schade & Michalke (1962) and by Michalke & Wille (1964) confirmed that for large Reynolds numbers the instability properties of free boundary layers are not noticeably affected by viscosity. Domm (1956) stated that some properties of the laminar-turbulent transition may be explained by the existence of vortices.

Benney (1961) investigated the influence of three-dimensional disturbances on the instability of a shear layer. He found a formation of longitudinal vortices, which become important in the non-linear range, even though his calculations were only performed for the neutral case. Such longitudinal vortex structure, however, has been found in wall boundary layers, for instance, on a flat plate by Klebanoff & Tidstrom (1958), but in free boundary layers the three-dimensional disturbances apparently become important only in the last stages of the transition process, as can be seen, for instance, on figure 27 of Wille (1963), in the free boundary layer of an axisymmetric jet.

Concerning the rolling-up of free boundary layers, only a few investigations are yet known. Rosenhead (1931), Birkhoff & Fisher (1959) as well as Hama & Burke (1960) calculated the rolling-up of a vortex sheet, which is the simplest case of a free-boundary-layer profile, approximately. Abernathy & Kronauer (1962), who also took vortex sheets, investigated the development of the Kármán vortex street in a wake. The rolling-up process of the linear shear layer, which is equivalent to a finite thick vortex sheet, was calculated approximately by Michalke (1963). In this case the initial disturbance of the vorticity was calculated by means of the inviscid linearized stability theory. The common basis of all the calculations concerning the rolling-up process is given by the method of replacing the continuously distributed vorticity of the disturbed velocity profile by a certain distribution of individual potential vortices, the motion of which is calculated by means of the induction law. Particularly in the last paper, the temporal development of the disturbed linear shear layer shows clearly the rolling-up process with a simultaneous concentration of the individual vortices in certain regions of the flow. Thus the formation of vortices in a disturbed free boundary layer is confirmed by the results in the framework of the simplifications used.

The results for the rolling-up obtained in this crude way, may, however, be far from giving a description of the real process, as the continuous vorticity distribution is approximated only by discrete potential vortices. Furthermore, the assumed velocity profiles—a 'jump' profile in the case of the vortex sheet and a 'broken-line' profile in the case of the linear shear layer—cannot be realized

experimentally. Therefore it seems to be of some importance to use a steadily curved velocity profile for theoretical investigations. Very simple in the analytical sense is the hyperbolic-tangent velocity profile. Using this profile in the following analysis, the vortex formation in a free boundary layer will be investigated according to stability theory.

2. The vorticity distribution of the disturbed hyperbolic-tangent velocity profile

The basic flow is assumed to be parallel and therefore only one velocity component $U(y)$ in the basic flow direction x exists. The y-axis is perpendicular to the x-axis. The basic velocity profile is given in dimensionless form by

$$U(y) = 0{\cdot}5\,[1 + \tanh y]. \tag{1}$$

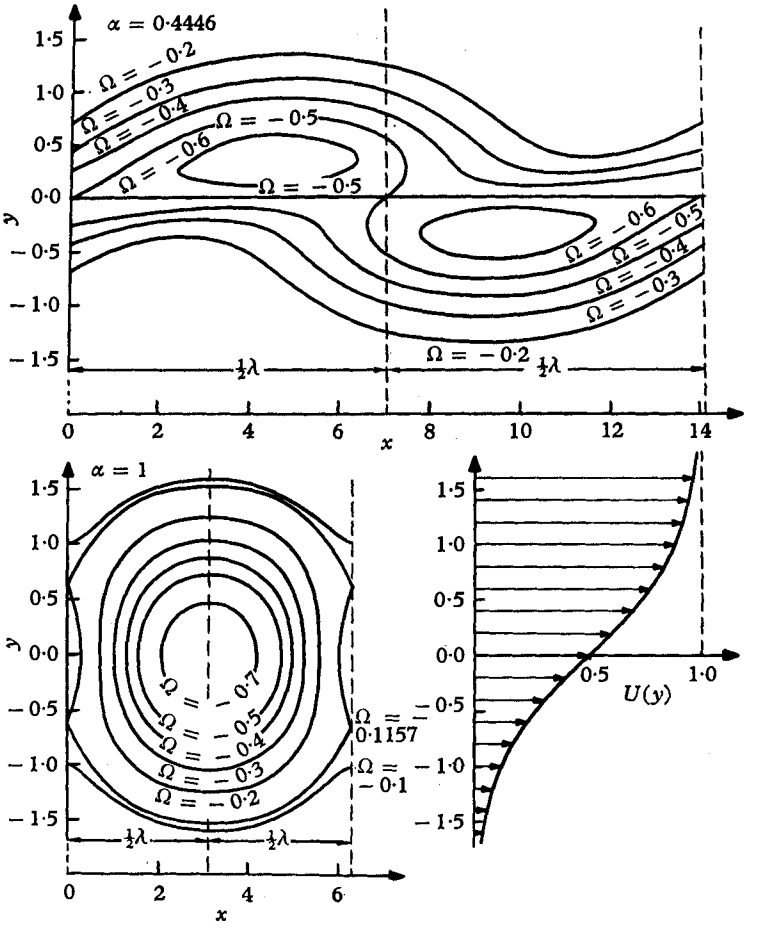

FIGURE 1. Lines of constant vorticity of the disturbed hyperbolic-tangent velocity profile for the wave-number $\alpha = 0{\cdot}4446$ of maximum amplification and $\alpha = 1$ of the neutral disturbance at the time $t = 0$ and a disturbance magnitude $\epsilon = 0{\cdot}2$ according to the inviscid linearized stability theory after Michalke (1964).

The corresponding undisturbed vorticity distribution $\Omega_0(y)$ for this velocity profile is defined by

$$\Omega_0(y) = -\frac{dU}{dy} = -0{\cdot}5\,\mathrm{sech}^2 y. \tag{2}$$

Stability calculations for the hyperbolic-tangent velocity profile according to the linearized theory were performed numerically by Betchov & Szewczyk (1963) as well as by Michalke (1964). Using the computed eigenvalues and eigenfunctions for the inviscid case, the physical properties of the disturbed flow were discussed in the latter paper. It was shown there that from a study of the streamlines no essential insight into the instability mechanism and the vortex formation is gained. For this reason the vorticity distribution of the disturbed flow was also calculated and discussed in that paper. Figure 1 shows lines of constant vorticity for the neutral disturbance (wave-number $\alpha = 1$) and for the most strongly amplified disturbance ($\alpha = 0{\cdot}4446$). The disturbance magnitude ϵ which can be chosen freely was assumed as relatively large in order to show the phenomenon more clearly. It is evident that a qualitative distinction between the neutral and the amplified disturbance exists. For the most strongly amplified disturbance two maxima of $|\Omega|$ are found within a disturbance wavelength λ, but only one maximum for the neutral disturbance.

If we interpret these concentrations of vorticity as 'vortices' in the above mentioned sense, it is obvious that in the neutral case the arrangement of vorticity corresponds essentially to a one-row vortex street. With respect to the mutual induction this arrangement is an equilibrium state of motion.

Yet in the case of amplified disturbances the arrangement of vorticity corresponds to two parallel vortex rows which are displaced relative to one another. Therefore an equilibrium state of motion exists no more. Both 'elementary vortices' within a wavelength will obviously have the tendency to rotate around their common centre or, taking the transport velocity into account, to slip around each other.

3. Temporal development of the disturbed flow

Another point of interest is the temporal development of the disturbed flow. The velocity field of the disturbed flow according to the inviscid linearized stability theory can be evaluated by means of the complex eigenfunctions $\phi(y)$ which are calculated by Michalke (1964). Thus we obtain for the velocity component in the basic flow direction

$$u = U(y) + \epsilon e^{\alpha c_i t}[\phi_r'(y)\cos\alpha(x - c_r t) - \phi_i'(y)\sin\alpha(x - c_r t)], \tag{3}$$

and the component normal to this

$$v = \epsilon\alpha e^{\alpha c_i t}[\phi_r(y)\sin\alpha(x - c_r t) + \phi_i(y)\cos\alpha(x - c_r t)]. \tag{4}$$

ϵ is again the disturbance magnitude, α the wave-number of the disturbance, c_r its phase velocity, and αc_i the disturbance growth rate. $\phi_r(y)$ and $\phi_i(y)$ denote the real and imaginary part of the complex eigenfunction.

Now, since the velocity field according to the inviscid linearized theory is determined, we can calculate the path line of any particle of the disturbed flow. The differential equation governing the motion of a particle is given by

$$\left.\begin{aligned} dx/dt &= u[x(t), y(t), t], \\ dy/dt &= v[x(t), y(t), t], \end{aligned}\right\} \tag{5}$$

where the right-hand sides are given by (3) and (4). $x(t)$ and $y(t)$ denote the positions of the particle at the time t.

It may be of special interest to obtain the positions of particles which were placed along straight lines parallel to the x-axis in the initial state. Lines connecting the positions of these particles at a later time are special 'material

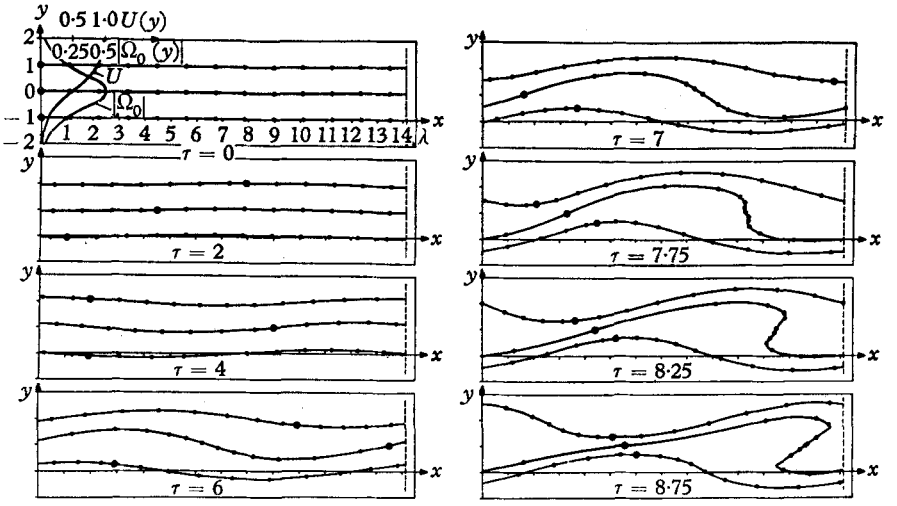

FIGURE 2. Temporal development of the disturbed hyperbolic-tangent velocity profile according to the inviscid linearized stability. Wave-number $\alpha = 0{\cdot}4446$ of maximum amplification; initial disturbance magnitude $\epsilon = 0{\cdot}01$; modified time $\tau = \alpha c_r t$.

lines' which may be called here simply 'limit lines', because all particles which were once inside a region limited by two different limit lines remain inside this region at all times. Experimentally the temporal development of a free boundary layer can be studied if a flow region limited by two different limit lines is visualized by smoke or dye.

For the most strongly amplified disturbance of the hyperbolic-tangent velocity profile, the temporal development of three limit lines was obtained by calculating the path lines of the particles. For this case the disturbance wave-number is $\alpha = 0{\cdot}4446$, the growth rate $\alpha c_i = 0{\cdot}09485$, and the phase velocity $c_r = 0{\cdot}5$.

Strictly the calculation should start at the time $t = -\infty$, where the disturbance tends to zero and only the basic flow remains. But, because of computational reasons, the calculation has to start at a finite time $t = t_0$. Therefore the effective disturbance magnitude at this time $t = t_0$ has the value $\epsilon \exp(\alpha c_i t_0) \ll 1$, if ϵ is

small enough so that the flow field differs only slightly from the undisturbed basic flow. Since ϵ can be chosen freely, we can assume $t_0 = 0$.

In the initial state the particles were positioned on the straight lines $y = 1$, $y = 0$ and $y = -1$, each having 13 particles per wavelength λ. The disturbance magnitude was chosen to be $\epsilon = 0{\cdot}01$. Figure 2 shows the result of the computation. The positions of the particles at the modified times

$$\tau = \alpha c_r t \tag{6}$$

are reduced to one wavelength. The particle originally first in each row is marked by a circle. It is obvious that with increasing time τ the boundary layer becomes thinner in certain regions and thicker in others. Furthermore, the medial limit line shows a tendency to roll up with a simultaneous concentration of particles. We have, therefore, to suppose that, if vortices are formed in free boundary layers, they should occur in the thicker part of the disturbed layer. Then a concentration of vorticity should be expected there. By comparing the vorticity distribution with the plot of the limit lines at the modified time $\tau = 7{\cdot}0210$, for instance, where $\epsilon \exp(c_i \tau / c_r) = 0{\cdot}2$, we see from figure 3 that there are, in fact, maximum values of vorticity in these parts of the free boundary layer.

4. Comparison between the results of the linearized and the non-linear theory

We must, however, keep in mind that for these relatively large times the assumptions of the linearized stability theory will surely no longer be valid. The instantaneous disturbance magnitude $\epsilon \exp(\alpha c_i t)$ increases exponentially in time and will reach high values quickly. At $\tau = 7{\cdot}0210$ the instantaneous disturbance magnitude becomes 20 times the initial disturbance magnitude. Therefore the non-linear equations should be used.

In the inviscid two-dimensional case the vorticity transport is described by the Helmholtz equation

$$\frac{d\Omega}{dt} = \frac{\partial \Omega}{\partial t} + u \frac{\partial \Omega}{\partial x} + v \frac{\partial \Omega}{\partial y} = 0. \tag{7}$$

From this equation it follows that, if a particle is moving along its path line, its vorticity remains constant for all times. For the undisturbed basic flow, however, the lines of constant vorticity $\Omega = \Omega_0 =$ constant are straight lines parallel to the x-axis and, therefore, they are identical with the chosen limit lines. In the inviscid case the limit lines also remain identical with the lines of constant vorticity for all times. Furthermore, if the vorticity of the undisturbed flow has an extremal value, it follows from the Helmholtz equation that this extremum of vorticity cannot be exceeded at any time. Thus we have a good criterion to examine the validity of the linearized theory.

In our calculations the limit lines initially positioned at $y = \pm 1$ are identical with the lines $\Omega_0 = -0{\cdot}21$ of the undisturbed vorticity, even though, because of the finite disturbance magnitude $\epsilon \exp(\alpha c_i t_0)$ in the initial state of the computation, the vorticity along these lines is not exactly constant, but changes in

order of magnitude of ϵ. The third limit line initially positioned at $y = 0$ corresponds to the line of extremal vorticity $\Omega_0 = -0{\cdot}5$, but for the same reason it does not remain exactly a line of extremal vorticity in the initial state of the

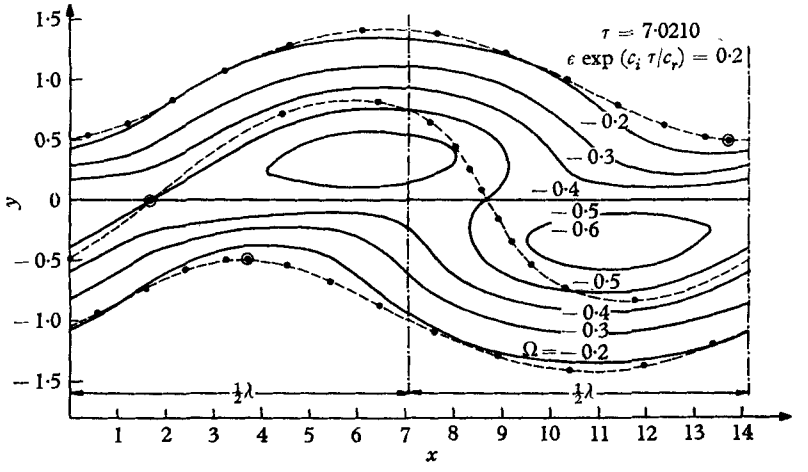

FIGURE 3. Comparison between the vorticity distribution and the limit lines of the disturbed hyperbolic-tangent velocity profile (linearized theory). Disturbance wavenumber $\alpha = 0{\cdot}4446$; initial disturbance magnitude $\epsilon = 0{\cdot}01$.

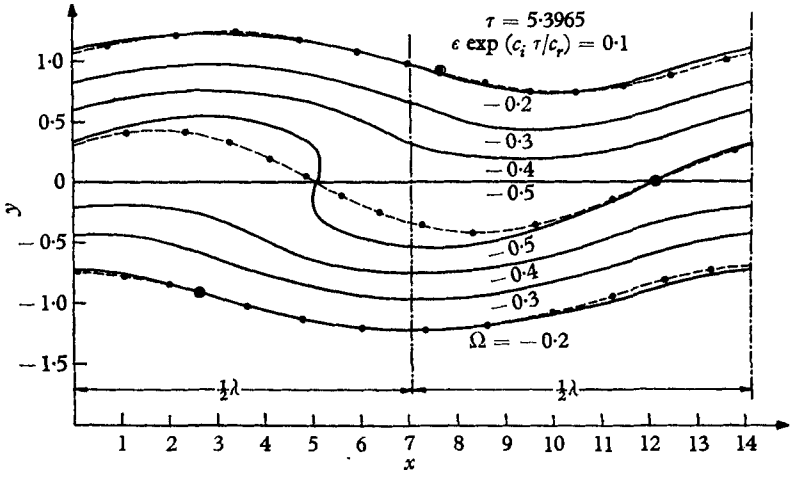

FIGURE 4. Comparison between the lines of constant vorticity and the limit lines of the disturbed hyperbolic-tangent velocity profile (linearized theory). Disturbance wavenumber $\alpha = 0{\cdot}4446$; initial disturbance magnitude $\epsilon = 0{\cdot}01$.

computation. This influence, however, may be neglected, because ϵ is sufficiently small. Looking at figure 4 we find for $\tau = 5{\cdot}3965$ where $\epsilon \exp(\alpha c_i t) = 0{\cdot}1$ both the outer limit lines show good agreement with the lines of constant vorticity $\Omega = -0{\cdot}20$. From this it follows that in these regions of the flow the linearized theory seems to be sufficient. Concerning the limit line initially positioned at the critical layer $y = 0$ we see, however, that the corresponding line of vorticity

$\Omega = -0{\cdot}5$ is split into two lines with a region of higher vorticity between them. Here we also find disagreement with the non-linear theory, as stated already by Lin (1958).

However, we are now in the position to describe how the vorticity distribution due to the non-linear development should look. The limit line placed initially in the critical layer must remain identical with the line of extremal vorticity, while the vorticity distribution outside the critical layer should be similar to that found by the linearized theory.

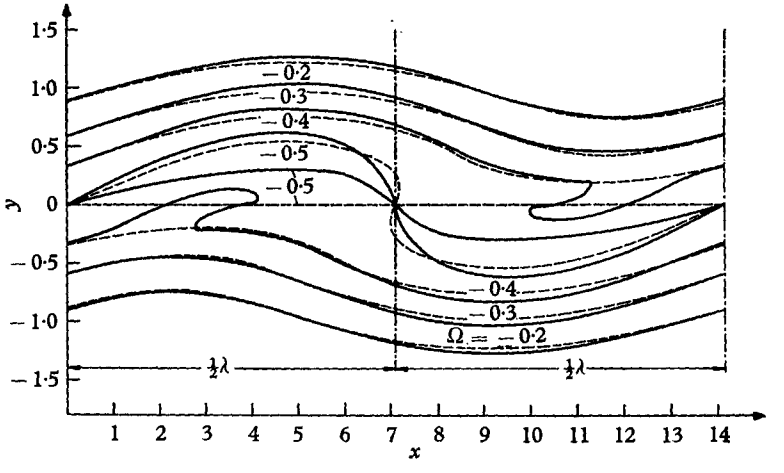

FIGURE 5. The vorticity distribution of the disturbed hyperbolic-tangent velocity profile due to the non-linear stability theory (third-order approximation) compared with that due to the linearized theory for maximum amplification ($\alpha = 0{\cdot}4446$); disturbance magnitude $|A| = 0{\cdot}1$. ———, Third-order approximation; – – – –, first-order approximation.

Obviously, a better agreement with the non-linear development must be expected with application of the non-linear stability theory according to Stuart (1961). Taking more and more terms of his series into account, the distance between both lines of initially extremal vorticity must decrease and, finally, both lines have to coalesce to a single one which has to be identical with the corresponding limit line. This tendency has also been confirmed by using Stuart's series up to the third-order terms (see appendix). Figure 5 shows the vorticity distribution as obtained in this way in comparison with the one due to the linearized theory. We see that, in fact, both lines of vorticity $\Omega = -0{\cdot}5$ are approaching each other. On the other hand, it is evident that in the inviscid case the third-order approximation is not sufficient in every respect for this instantaneous disturbance magnitude $|A| = 0{\cdot}1$. Therefore we may suppose that the convergence of Stuart's series is not very good in the inviscid case.

Finally, let us speculate how the vorticity distribution of a fully-developed vortex in a free boundary layer might look. It is assumed that the lines of constant vorticity will roll up in the inviscid case as in figure 6. The vorticity distribution across a vortex will be as shown below at the right and the distribution between two consecutive vortices as shown at the left. We see that we may find a concentration of vorticity in the vortex without an increase of the extremal value of

the vorticity Ω_{max}. Taking the viscosity into account the peaks and valleys of the vorticity in and between the vortices may be smoothed, as is shown by the dashed line, especially in the regions of large gradient changes. Thus we have to expect a vorticity distribution in the vortex which is similar to that of the Hamel–Oseen vortex. This is well confirmed by the computation of Amsden & Harlow (1964) who dealt with the non-linear development of a viscous shear layer by solving the viscous non-linear equations by a difference method. This may also be an explanation for the good agreement with experimental results as found by Timme (1957) and by Berger (1964) who calculated the flow pattern of a Kármán vortex street using Hamel–Oseen vortices for an approximation. Summarizing, we can say that the vortex formation in free boundary layers may be well described by means of the stability theory.

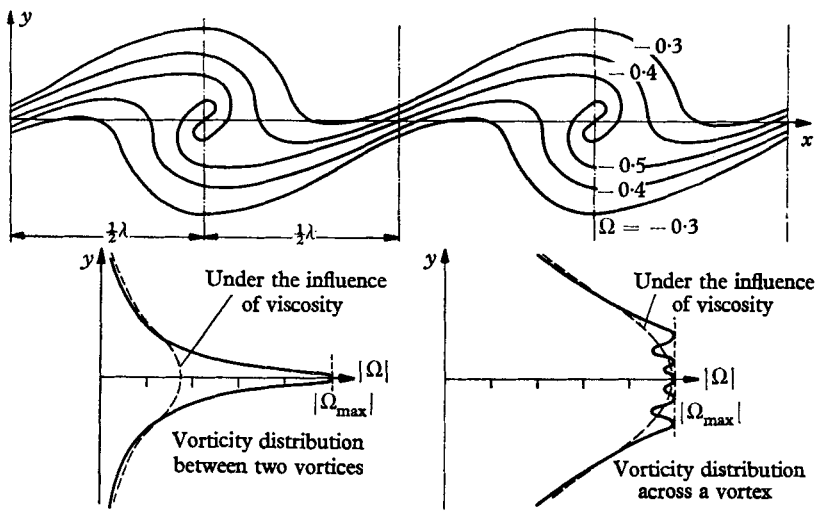

FIGURE 6. Vorticity distribution expected in a free boundary layer during rolling-up (inviscid non-linear theory).

Appendix. Application of Stuart's non-linear stability theory

The non-linear stability theory by Stuart (1961) has been applied to the tanh velocity profile. To simplify the writing of the formulae, the method has been modified somewhat by using the vorticity transport equation. For viscous two-dimensional flow this equation is

$$\frac{\partial \Omega}{\partial t} + \frac{\partial \psi}{\partial y}\frac{\partial \Omega}{\partial x} - \frac{\partial \psi}{\partial x}\frac{\partial \Omega}{\partial y} - \frac{1}{R}\Delta\Omega = 0, \tag{8}$$

where R denotes the Reynolds number. $\psi(x, y, t)$ is the stream function and $\Omega(x, y, t)$ the z-component of the vorticity defined by

$$\operatorname{curl} \mathbf{c} = \{0, 0, \Omega\}, \tag{9}$$

where

$$\mathbf{c} = \{u, v, 0\} = \left\{\frac{\partial \psi}{\partial y}, -\frac{\partial \psi}{\partial x}, 0\right\} \tag{10}$$

is the velocity vector. From (9) the vorticity follows as

$$\Omega = \frac{\partial v}{\partial x} - \frac{\partial u}{\partial y} = -\Delta\psi. \tag{11}$$

According to the method of Stuart, we look for a solution of the partial-differential-equation system (8) and (11) by using Fourier-series in x-direction:

$$\psi(x,y,t) = \mathscr{R}\left\{\sum_{\nu=0}^{\infty}\psi_\nu e^{\nu i\alpha x}\right\} = \frac{1}{2}\sum_{\nu=0}^{\infty}\{\psi_\nu(y,t)\,e^{\nu i\alpha x} + \tilde{\psi}_\nu(y,t)\,e^{-\nu i\alpha x}\}, \tag{12}$$

$$\Omega(x,y,t) = \mathscr{R}\left\{\sum_{\nu=0}^{\infty}\Omega_\nu e^{\nu i\alpha x}\right\} = \frac{1}{2}\sum_{\nu=0}^{\infty}\{\Omega_\nu(y,t)\,e^{\nu i\alpha x} + \tilde{\Omega}_\nu(y,t)\,e^{-\nu i\alpha x}\}. \tag{13}$$

The functions ψ_ν and Ω_ν are generally complex and the symbol $\sim$ denotes a complex conjugate.

By substituting (12) and (13) in (8) and (11) and by separation of the harmonic components, we obtain in a way similar to Watson's (1960) for $\nu = 0$

$$\frac{\partial\overline{\Omega}_0}{\partial t} + \frac{i\alpha}{4}\sum_{\mu=1}^{\infty}\mu\frac{\partial}{\partial y}[\Omega_\mu\tilde{\psi}_\mu - \tilde{\Omega}_\mu\psi_\mu] - \frac{1}{R}\frac{\partial^2\overline{\Omega}_0}{\partial y^2} = 0, \tag{14}$$

$$\overline{\Omega}_0 = -\partial^2\overline{\psi}_0/\partial y^2. \tag{15}$$

The zero-order terms are marked by a bar, as they represent mean values of the flow with respect to x. For $\nu \geqslant 1$ we obtain

$$\left[\overline{U} - \frac{i}{\nu\alpha}\frac{\partial}{\partial t}\right]\Omega_\nu + \overline{U}''\psi_\nu + \frac{i}{\nu\alpha R}\left[\frac{\partial^2\Omega_\nu}{\partial y^2} - \nu^2\alpha^2\,\Omega_\nu\right]$$
$$= \frac{1}{2\nu}\left\{\sum_{\mu=1}^{\nu-1}\mu\left[\psi_\mu\frac{\partial\Omega_{\nu-\mu}}{\partial y} - \Omega_\mu\frac{\partial\psi_{\nu-\mu}}{\partial y}\right] + \sum_{\mu=\nu+1}^{\infty}\mu\left[\psi_\mu\frac{\partial\tilde{\Omega}_{\mu-\nu}}{\partial y} - \Omega_\mu\frac{\partial\tilde{\psi}_{\mu-\nu}}{\partial y}\right]\right.$$
$$\left. + \sum_{\mu=\nu+1}^{\infty}(\mu-\nu)\left[\tilde{\Omega}_{\mu-\nu}\frac{\partial\psi_\mu}{\partial y} - \tilde{\psi}_{\mu-\nu}\frac{\partial\Omega_\mu}{\partial y}\right]\right\}, \tag{16}$$

$$\Omega_\nu = -\left[\frac{\partial^2\psi_\nu}{\partial y^2} - \nu^2\alpha^2\psi_\nu\right], \tag{17}$$

where $\overline{U}$ stands for

$$\overline{U} = \partial\overline{\psi}_0/\partial y, \tag{18}$$

and

$$\overline{U}'' = -\partial\overline{\Omega}_0/\partial y. \tag{19}$$

The following expansion is compatible with equations (14) to (17)

$$\left.\begin{aligned} \overline{U} &= U + |A|^2\,\overline{u}^{(1)} + \ldots, & \overline{\Omega}_0 &= \Omega_0 + |A|^2\,\overline{\omega}^{(1)} + \ldots, \\ \psi_1 &= A[\phi_1 + |A|^2\,\phi_1^{(1)} + \ldots, & \Omega_1 &= A[\omega_1 + |A|^2\,\omega_1^{(1)} + \ldots, \\ \psi_2 &= A^2[\phi_2 + \ldots, & \Omega_2 &= A^2[\omega_2 + \ldots, \\ \psi_3 &= A^3[\phi_3 + \ldots, & \Omega_3 &= A^3[\omega_3 + \ldots, \end{aligned}\right\} \tag{20}$$

if the complex time-dependent amplitude function $A = A(t)$ satisfies the differential equation

$$dA/dt = A[a_0 + a_1|A|^2 + \ldots], \tag{21}$$

and if all the other functions depend only on y. $U(y)$ denotes the given basic velocity profile and $\Omega_0 = -U'$ the corresponding vorticity distribution. a_1 is the so-called first Landau constant.

Inserting (20) into (14) to (17) we can arrange the terms in powers of A. With the conventional notation

$$a_0 = -i\alpha c = -i\alpha(c_r + ic_i), \tag{22}$$

we obtain the following ordinary differential equations at $A(t)$

$$\left.\begin{aligned}(U-c)\,\omega_1+U''\phi_1+\frac{i}{\alpha R}(\omega_1''-\alpha^2\omega_1)&=0,\\ \omega_1&=-(\phi_1''-\alpha^2\phi_1),\end{aligned}\right\} \tag{23}$$

at $|A|^2$

$$\left.\begin{aligned}2c_i\bar{\omega}^{(1)}-\frac{1}{\alpha R}\bar{\omega}^{(1)''}&=\tfrac{1}{2}\mathscr{R}\{i(\phi_1\tilde{\omega}_1)'\},\\ \bar{\omega}^{(1)}&=-\bar{u}^{(1)'},\end{aligned}\right\} \tag{24}$$

at A^2

$$\left.\begin{aligned}(U-c)\,\omega_2+U''\phi_2+\frac{i}{2\alpha R}(\omega_2''-4\alpha^2\omega_2)&=\tfrac{1}{4}(\phi_1\omega_1'-\omega_1\phi_1'),\\ \omega_2&=-(\phi_2''-4\alpha^2\phi_2),\end{aligned}\right\} \tag{25}$$

at $A|A|^2$

$$\left.\begin{aligned}[U-c_3]\,\omega_1^{(1)}+U''\phi_1^{(1)}+\frac{i}{\alpha R}[\omega_1^{(1)''}-\alpha^2\omega_1^{(1)}]&=\frac{ia_1}{\alpha}\omega_1-\bar{u}^{(1)}\omega_1+\bar{\omega}^{(1)'}\phi_1\\ &\quad+\phi_2\tilde{\omega}_1'-\omega_2\tilde{\phi}_1'+\tfrac{1}{2}[\tilde{\omega}_1\phi_2'-\tilde{\phi}_1\omega_2'],\\ \omega_1^{(1)}&=-[\phi_1^{(1)''}-\alpha^2\phi_1^{(1)}],\end{aligned}\right\} \tag{26}$$

with $c_3=c_r+i3c_i$, and at A^3

$$\left.\begin{aligned}[U-c]\,\omega_3+U''\phi_3+\frac{i}{3\alpha R}[\omega_3''-9\alpha^2\omega_3]&=\tfrac{1}{6}[\phi_1\omega_2'-\omega_1\phi_2'+2(\phi_2\omega_1'-\omega_2\phi_1')],\\ \omega_3&=-[\phi_3''-9\alpha^2\phi_3],\end{aligned}\right\} \tag{27}$$

and so on. Equation (23) represents the Orr–Sommerfeld equation of the linearized stability theory.

Taking terms up to the third order in A into account the solution of equation (21) can be found in a closed form. With the initial value

$$A(0)=\epsilon \tag{28}$$

as a measure for the disturbance magnitude, the integration yields for $a_{1i}=0$

$$A(t)=\frac{\epsilon e^{-i\alpha ct}}{\sqrt{\{1+(-a_{1r}/\alpha c_i)\,\epsilon^2(e^{2\alpha c_i t}-1)\}}}. \tag{29}$$

For the special case $c_i=0$ the solution becomes

$$\lim_{c_i\to 0}A(t)=\frac{\epsilon e^{-i\alpha c_r t}}{\sqrt{\{1+(-a_{1r})\,\epsilon^2(2t)\}}}. \tag{30}$$

Using only the first-order terms in A, i.e. $a_1=0$, we obtain the result of the linearized stability theory:

$$\lim_{a_1\to 0}A(t)=\epsilon e^{-i\alpha ct}. \tag{31}$$

For the present problem of the hyperbolic-tangent velocity profile (1), the solutions of (23) have been computed numerically for the inviscid case ($R^{-1}=0$) by Michalke (1964). By these results the remaining equations (24) to (27) can be solved successively as a boundary-value problem. The boundary values are in this case determined by the conditions that the disturbances $\psi_\nu(y,t)$ must vanish

for $y \to \pm\infty$. The calculation was performed numerically with a LGP 30 computer up to the third-order terms for the most strongly amplified disturbance and $R^{-1} = 0$. Then the disturbance wave-number is

$$\alpha = 0{\cdot}4446, \tag{32}$$

and the eigenvalue

$$c = 0{\cdot}5 + 0{\cdot}2133i. \tag{33}$$

The up to now undetermined first Landau constant a_1 remains undetermined for amplified disturbances with $c_i \neq 0$. Since $c_3 \neq c$, the homogeneous equation (26) is different from (23) and has no solution satisfying the boundary conditions. Thus for every value of a_1 a solution of the inhomogeneous equation (26) can be found which satisfies the boundary conditions. Only, if c_i is zero, we have $c_3 = c$ and a solution of (26) satisfying the boundary conditions can only be obtained for a special value of a_1. Therefore the Landau constant a_1 calculated for the neutral case is believed to be significant for amplified disturbances too. The value of this constant for the tanh velocity profile was found by Schade (1964) to be

$$a_1 = a_{1r} = -16/3\pi. \tag{34}$$

Knowing all terms of (13) up to $\nu = 3$, the lines of constant vorticity have been computed with the assumption $|A| = 0{\cdot}1$. The results are shown in figure 5.

This investigation was done at the Institut für Turbulenzforschung of the Deutsche Versuchsanstalt für Luft- und Raumfahrt e.V. at Berlin. The author wishes to express his gratitude to Professor Dr-Ing. R. Wille, the Director of the Institute, and to Dr-Ing. H. Schade for many stimulating discussions. The Deutsche Forsuchungsgemeinschaft, Bad Godesberg, kindly gave financial support for the numerical computations. The author is also much indebted to the Deutsche Versuchanstalt für Luft- und Raumfahrt and to the International Union for Theoretical and Applied Mechanics and the U.S. Sponsors for enabling him to present this paper at the IUTAM Symposium, *On Concentrated Vortex Motions in Fluids*, at Ann Arbor, Mich. in July 1964.

REFERENCES

Abernathy, F. H. & Kronauer, R. E. 1962 *J. Fluid Mech.* **13**, 1.

Amsden, A. A. & Harlow, F. H. 1964 *Phys. Fluids*, **7**, 327.

Benney, D. J. 1961 *J. Fluid Mech.* **10**, 209.

Berger, E. 1964 *Z. Flugwiss.* **12**, 41.

Betchov, R. & Szewczyk, A. 1963 *Phys. Fluids*, **6**, 1391.

Birkhoff, G. & Fisher, J. 1959 *Rend. Circ. Math. Palermo*, Ser. 2, **8**, 77.

Domm, U. 1956 *Deutsche Versuchsanstalt f. Luftfahrt, Porz-Wahn*, DVL-*Rep.* no. 26.

Esch, R. E. 1957 *J. Fluid Mech.* **3**, 289.

Hama, F. R. & Burke, E. R. 1960 *Inst. Fluid Dynam. Appl. Math., Univ. Maryland, Tech. Note* BN-220.

Helmholtz, H. 1868 *Monatsbericht, Königl. Akad. Wiss., Berlin*, 215–28.

Klebanoff, P. S. & Tidstrom, K. D. 1958 *Nat. Bur. Stand. Rep.* 5741.

Lessen, M. 1950 *Nat. Adv. Comm. Aero., Wash., Tech. Rep.* no. 979.

Lin, C. C. 1955 *The Theory of Hydrodynamic Stability*. Cambridge University Press.

LIN, C. C. 1958 *Boundary Layer Research* (ed. H. Görtler), pp. 144–57. Berlin: Springer-Verlag.

MICHALKE, A. 1963 *AFOSR Tech. Note* no. 2, Contract AF 61(052)-412. Also 1964 *Ing. Arch.* **33**, 264.

MICHALKE, A. 1964 *J. Fluid Mech.* **19**, 543.

MICHALKE, A. & WILLE, R. 1964 *Verhandl. XI. Internat. Kongr. Angew. Mech.* Berlin: Springer-Verlag (to be published).

RAYLEIGH, LORD 1880 *Sci. Papers*, **1**, 474–87.

ROSENHEAD, L. 1931 *Proc. Roy. Soc.* A, **134**, 170.

SATO, H. 1960 *J. Fluid Mech.* **7**, 53.

SCHADE, H. 1964 *Phys. Fluids*, **7**, 623.

SCHADE, H. & MICHALKE, A. 1962 *Z. Flugwiss.* **10**, 147. Also *AFOSR Tech. Note* no. 3191.

STUART, J. T. 1961 *Adv. Aero. Sci.* **3–4**, 121–42.

TATSUMI, T. & KAKUTANI, T. 1958 *J. Fluid Mech.* **4**, 261.

TIMME, A. 1957 *Ing. Arch.* **25**, 205.

WATSON, J. 1960 *J. Fluid Mech.* **9**, 371.

WILLE, R. 1963 *Z. Flugwiss.* **11**, 222.